

Efficient Competitive Self-Play Policy Optimization

Yuanyi Zhong¹ Yuan Zhou² Jian Peng¹
 yuanyiz2@illinois.edu yuanz@illinois.edu jianpeng@illinois.edu

¹ Department of Computer Science

² Department of Industrial and Enterprise Systems Engineering
 University of Illinois at Urbana-Champaign

Abstract: Reinforcement learning from self-play has recently reported many successes. Self-play, where the agents compete with themselves, is often used to generate training data for iterative policy improvement. In previous work, heuristic rules are designed to choose an opponent for the current learner. Typical rules include choosing the latest agent, the best agent, or a random historical agent. However, these rules may be inefficient in practice and sometimes do not guarantee convergence even in the simplest matrix games. In this paper, we propose a new algorithmic framework for competitive self-play reinforcement learning in two-player zero-sum games. We recognize the fact that the Nash equilibrium coincides with the saddle point of the stochastic payoff function, which motivates us to borrow ideas from classical saddle point optimization literature. Our method trains several agents simultaneously, and intelligently takes each other as opponent based on simple adversarial rules derived from a principled perturbation-based saddle optimization method. We prove theoretically that our algorithm converges to an approximate equilibrium with high probability in convex-concave games under standard assumptions. Beyond the theory, we further show the empirical superiority of our method over baseline methods relying on the aforementioned opponent-selection heuristics in matrix games, grid-world soccer, Gomoku, and simulated robot sumo, with neural net policy function approximators.

Keywords: self-play, policy optimization, two-player zero-sum game, multiagent

1 Introduction

Reinforcement learning (RL) from self-play has drawn tremendous attention over the past few years. Empirical successes have been observed in several challenging tasks, including Go [1, 2, 3], simulated hide-and-seek [4], simulated sumo wrestling [5], Capture the Flag [6], Dota 2 [7], StarCraft II [8], and poker [9], to name a few. During RL from self-play, the learner collects training data by competing with an opponent selected from its past self or an agent population. Self-play presumably creates an auto-curriculum for the agents to learn at their own pace. At each iteration, the learner always faces an opponent that is comparably in strength to itself, allowing continuous improvement.

The way the opponents are selected often follows human-designed heuristic rules in prior works. For example, AlphaGo [1] always competes with the latest agent, while the later generation AlphaGo Zero [2] and AlphaZero [3] generate self-play data with the maintained best historical agent. In specific tasks, such as OpenAI’s sumo wrestling environment, competing against a randomly chosen historical agent leads to the emergence of more diverse behaviors [5] and more stable training than against the latest agent [10]. In population-based training [6, 11] and AlphaStar [8], an elite or random agent is picked from the agent population as the opponent.

Unfortunately, these rules may be inefficient and sometimes ineffective in practice and do not necessarily enjoy convergence guarantee to the “average-case optimal” solution even in tabular matrix games. In fact, in the simple Matching Pennies game, self-play with the latest agent fails to converge and falls into an oscillating behavior, as shown in Sec. 5.

In this paper, we want to develop an algorithm that adopts a principally-derived opponent-selection rule to alleviate some of the issues mentioned above. This requires clarifying first what the solution of self-play RL should be. From the game-theoretical perspective, Nash equilibrium is a funda-

mental solution concept that characterizes the desired “average-case optimal” strategies (policies). When each player assumes other players also play their equilibrium strategies, no one in the game can gain more by unilaterally deviating to another strategy. Nash, in his seminal work [12], has established the existence result of mixed-strategy Nash equilibrium of any finite game. Thus solving for a mixed-strategy Nash equilibrium is a reasonable goal of self-play RL.

We consider the particular case of two-player zero-sum games, a reasonable model for the competitive environments studied in the self-play RL literature. In this case, the Nash equilibrium is the same as the (global) saddle point and as the solution of the minimax program $\min_{x \in X} \max_{y \in Y} f(x, y)$. We denote x, y as the strategy profiles (in RL language, policies) and f as the loss for x or utility/reward for y . A saddle point $(x^*, y^*) \in X \times Y$, where X, Y are the sets of all possible mixed-strategies (stochastic policies) of the two players, satisfies the following key property

$$f(x^*, y) \leq f(x^*, y^*) \leq f(x, y^*), \forall x \in X, \forall y \in Y. \quad (1)$$

Connections to the saddle point problem and game theory inspire us to borrow ideas from the abundant literature for finding saddle points in the optimization field [13, 14, 15, 16] and for finding equilibrium in the game theory field [17, 18, 19]. One particular class of method, i.e., the perturbation-based subgradient methods to find the saddles [14, 15], is especially appealing. This class of method directly builds upon the inequality properties in Eq. 1, and has several advantages: (1) Unlike some algorithms that require knowledge of the game dynamic [1, 2, 20], it requires only subgradients; thus, it is easy to adapt to policy optimization with estimated policy gradients. (2) It is guaranteed to converge in its last iterate instead of an average iterate, hence alleviates the need to compute any historical averages as in [18, 19, 17], which can get complicated when neural nets are involved [21]. (3) Most importantly, it prescribes a simple principled way to adversarially choose opponents, which can be naturally implemented with a concurrently-trained agent population.

To summarize, we adapt the perturbation-based methods of classical saddle point optimization into the model-free self-play RL regime. This results in a novel population-based policy gradient method for competitive self-play RL described in Sec. 3. Analogous to the standard model-free RL setting, we assume only “naive” players [22] where the game dynamic is hidden and only rewards for their own actions are revealed. This enables broader applicability than many existing algorithms [1, 2, 20] to problems with mismatched or unknown game dynamics, such as many real-world or simulated robotic problems. In Sec. 4, we provide an approximate convergence theorem of the proposed algorithm for convex-concave games as a sanity check. Sec. 5 shows extensive experiment results favoring our algorithm’s effectiveness on several games, including matrix games, a game of grid-world soccer, a board game, and a challenging simulated robot sumo game. Our method demonstrates better per-agent sample efficiency than baseline methods with alternative opponent-selection rules. Our trained agents can also outperform the agents trained by other methods on average.

2 Related Work

Reinforcement learning trains a single agent to maximize the expected return through interacting with an environment [23]. Multiagent reinforcement learning (MARL), where two-agent is a special case, concerns multiple agents taking actions in the same environment [24]. Self-play is a training paradigm to generate data for learning in MARL and has led to great successes, achieving superhuman performance in many domains [25, 1, 9]. Applying RL algorithms naively as independent learners in MARL sometimes produces strong agents [25], but often does not converge to the equilibrium. People have studied ways to extend RL algorithms to MARL, e.g., minimax-Q [24], Nash-Q [26], WoLF-PG [27], etc. However, most of these methods are designed for tabular RL only therefore not readily applicable to continuous state action spaces and complex policy functions where gradient-based policy optimization methods are preferred. Very recently, there is some work on the non-asymptotic regret analysis of tabular self-play RL [28]. While our work roots from a practical sense, these work enrich the theoretical understanding and complement ours.

There are algorithms developed from the game theory and online learning perspective [29, 20, 30], notably Tree search, Fictitious self-play [18] and Regret minimization [22, 17], and Mirror descent [31, 32]. Tree search such as minimax and alpha-beta pruning is particularly effective in small-state games. Monte Carlo Tree Search (MCTS) is also effective in Go [1]. However, Tree search requires learners to know the exact game dynamics. The latter ones typically require maintaining some historical quantities. In Fictitious play, the learner best responds to a historical average opponent,

and the average strategy converges. Similarly, the total historical regrets in all (information) states are maintained in (counterfactual) regret minimization [17]. The extragradient rule in [31] is a special case of the adversarial perturbation we rely on in this paper. Most of those algorithms are designed only for discrete state action environments. Special care has to be taken with neural net function approximators [21]. On the contrary, our method enjoys last-iterate convergence under proper convex-concave assumptions, does not require the complicated computation of averaging neural nets, and is readily applicable to continuous environments through policy optimization.

In two-player zero-sum games, the Nash equilibrium coincides with the saddle point. This enables the techniques developed for finding saddle points. While some saddle-point methods also rely on time averages [16], a class of perturbation-based gradient method is known to converge under mild convex-concave assumption for deterministic functions [15, 14, 33]. We develop an efficient sampling version of them for stochastic RL objectives, which leads to a more principled and effective way of choosing opponents in self-play. Our adversarial opponent-selection rule bears a resemblance to [34]. However, the motivation of our work (and so is our algorithm) is to improve self-play RL, while [34] aims at attacking deep self-play RL policies. Though the algorithm presented here builds upon policy gradient, the same framework may be extended to other RL algorithms such as MCTS due to a recent interpretation of MCTS as policy optimization [35]. Finally, our way of leveraging Eq. 1 in a population may potentially work beyond gradient-based RL, e.g., in training generative adversarial networks similarly to [33] because of the same minimax formulation.

3 Method

Classical game theory defines a two-player zero-sum game as a tuple (X, Y, f) where X, Y are the sets of possible strategies of Players 1 and 2 respectively, and $f: X \times Y \mapsto \mathbb{R}$ is a mapping from a pair of strategies to a real-valued utility/reward for Player 2. The game is zero-sum (fully competitive), and Player 1’s reward is $-f$.

We consider mixed strategies (corresponding to stochastic policies in RL). In the discrete case, X and Y could be all probability distributions over the sets of actions. When parameterized function approximators are used, X, Y can be the spaces of all policy parameters.

Multiagent RL formulates the problem as a Stochastic Game [36], an extension to Markov Decision Processes (MDP). Denote a_t as the action of Player 1 and b_t as the action of Player 2 at time t , let T be the time limit of the game, then the stochastic payoff f writes as

$$f(x, y) = \mathbb{E}_{\substack{a_t \sim \pi_x, b_t \sim \pi_y, \\ s_{t+1} \sim P(\cdot | s_t, a_t, b_t)}} \left[\sum_{t=0}^T \gamma^t r(s_t, a_t, b_t) \right]. \quad (2)$$

The state sequence $\{s_t\}_{t=0}^T$ follows a transition dynamic $P(s_{t+1} | s_t, a_t, b_t)$. Actions are sampled according to stochastic policies $\pi_x(\cdot | s_t)$ and $\pi_y(\cdot | s_t)$. And $r(s_t, a_t, b_t)$ is the reward (payoff) for Player 2 at time t , determined jointly by the state and actions. We use the term ‘agent’ and ‘player’ interchangeably. In deep RL, x and y are the policy neural net parameters. In some cases [1], we can enforce $x = y$ by sharing parameters if the game is impartial or we do not want to distinguish them. The discounting factor γ weights short and long term rewards and is optional. Note that when one agent is fixed - taking y as an example - the problem x is facing reduces to an MDP, if we define a new state transition dynamic $P_{\text{new}}(s_{t+1} | s_t, a_t) = \sum_{b_t} P(s_{t+1} | s_t, a_t, b_t) \pi_y(b_t | s_t)$ and a new reward $r_{\text{new}}(s_t, a_t) = \sum_{b_t} r(s_t, a_t, b_t) \pi_y(b_t | s_t)$.

The naive algorithm provably works in strictly convex-concave games (where f is strictly convex in x and strictly concave in y) under assumptions in [13]. However, in general, it does not enjoy last-iterate convergence to the Nash equilibrium. Even for simple games such as Matching Pennies and Rock Paper Scissors, as we shall see in our experiments, the naive algorithm generates cyclic sequences of x^k, y^k that orbit around the equilibrium. This motivates us to study the perturbation-based method that converges under weaker assumptions.

Recall that the Nash equilibrium has to satisfy the saddle constraints Eq. 1: $f(x^*, y) \leq f(x^*, y^*) \leq f(x, y^*)$. The perturbation-based method builds upon this property [16, 15, 14] and directly optimize for a solution that meets the constraints. They find perturbed points u of x and v of y , and use gradients at (x, v) and (u, y) to optimize x and y . Under some regularity assumptions, gradient direction from a single perturbed point is adequate for proving convergence [16] for (not strictly)

Algorithm 1: Perturbation-based self-play policy optimization of an n agent population.

Input: N : number of iterations, η_k : learning rates, m_k : sample size, n : population size, l : number of inner policy updates;
Result: n pairs of policies;

- 1 Initialize $(x_i^0, y_i^0), i = 1, 2, \dots, n$;
- 2 **for** $k = 0, 1, 2, \dots, N - 1$ **do**
- 3 Evaluate $\hat{f}(x_i^k, y_j^k), \forall i, j \in 1 \dots n$ with Eq. 4 and sample size m_k ;
- 4 **for** $i = 1, \dots, n$ **do**
- 5 Construct candidate opponent sets $C_{y_i}^k = \{y_j^k : j = 1 \dots n\}$ and $C_{x_i}^k = \{x_j^k : j = 1 \dots n\}$;
- 6 Find perturbed $v_i^k = \arg \max_{y \in C_{y_i}^k} \hat{f}(x_i^k, y)$, perturbed $u_i^k = \arg \min_{x \in C_{x_i}^k} \hat{f}(x, y_i^k)$;
- 7 Invoke a single-agent RL algorithm (e.g., A2C, PPO) on x_i^k for l times that:
- 8 Estimate policy gradients $\hat{g}_{x_i}^k = \hat{\nabla}_x f(x_i^k, v_i^k)$ with sample size m_k (e.g., Eq. 5);
- 9 Update policy by $x_i^{k+1} \leftarrow x_i^k - \eta_k \hat{g}_{x_i}^k$ (or RmsProp);
- 10 Invoke a single-agent RL algorithm (e.g., A2C, PPO) on y_i^k for l times that:
- 11 Estimate policy gradients $\hat{g}_{y_i}^k = \hat{\nabla}_y f(u_i^k, y_i^k)$ with sample size m_k ;
- 12 Update policy by $y_i^{k+1} \leftarrow y_i^k + \eta_k \hat{g}_{y_i}^k$ (or RmsProp);
- 13 **return** $\{(x_i^N, y_i^N)\}_{i=1}^n$;

convex-concave functions. They can be easily extended to accommodate gradientbased policy optimization and stochastic RL objective Eq. 4.

We propose to find the perturbations from an agent population, resulting in the algorithm outlined in Alg. 1. The algorithm trains n pairs of agents simultaneously. The n^2 pairwise competitions are run as the evaluation step (Alg. 1 Line 3), costing $n^2 m_k$ trajectories. To save sample complexity, we may use these rollouts to do one policy update as well. Then a simple adversarial rule (Eq. 3) is adopted in Alg. 1 Line 6 to choose the opponents adaptively. The intuition is that v_i^k and u_i^k are the most challenging opponents in the population that the current x_i and y_i are facing.

$$v_i^k = \arg \max_{y \in C_{y_i}^k} \hat{f}(x_i^k, y), \quad u_i^k = \arg \min_{x \in C_{x_i}^k} \hat{f}(x, y_i^k). \quad (3)$$

The perturbations v_i^k and u_i^k always satisfy $f(x_i^k, v_i^k) \geq f(u_i^k, y_i^k)$, since $\max_{y \in C_{y_i}^k} \hat{f}(x_i^k, y) \geq \hat{f}(x_i^k, y_i^k) \geq \min_{x \in C_{x_i}^k} \hat{f}(x, y_i^k)$. Then we run gradient descent on x_i^k with the perturbed v_i^k as opponent to minimize $f(x_i^k, v_i^k)$, and run gradient ascent on y_i^k to maximize $f(u_i^k, y_i^k)$. Intuitively, the duality gap between $\min_x \max_y f(x, y)$ and $\max_y \min_x f(x, y)$, approximated by $f(x_i^k, v_i^k) - f(u_i^k, y_i^k)$, is reduced, leading to (x_i^k, y_i^k) converging to the saddle point (equilibrium).

We build the candidate opponent sets in Line 5 of Alg. 1 simply as the concurrently-trained n -agent population. Specifically, $C_{y_i}^k = \{y_1^k, \dots, y_n^k\}$ and $C_{x_i}^k = \{x_1^k, \dots, x_n^k\}$. This is due to the following considerations. An alternative source of candidates is the fixed known agents such as a rule-based agent, which may be unavailable in practice. Another source is the extragradient methods [14, 31], where extra gradient steps are taken on y before optimizing x . The extragradient method can be thought of as a local approximation to Eq. 3 with a neighborhood candidate opponent set, and thus related to our method. However, this method could be less efficient because the trajectory sample used in the extragradient estimation is wasted as it does not contribute to actually optimizing y . Yet another source could be the past agents. This choice is motivated by Fictitious play and ensures that the current learner always defeats a past self. But, as we shall see in the experiment section, self-play with a random past agent learns slower than our strategy. We expect all agents in the population in our algorithm to be strong, thus provide stronger learning signals.

Finally, we use Monte Carlo estimates to compute the values and gradients of f . In the classical game theory setting, the game dynamic and payoff are known, so it is possible to compute the exact values and gradients of $f(x, y)$. But this is a rather restricted setting. In model-free MARL, we have to collect roll-out trajectories to estimate both the function values through policy evaluation and gradients through Policy gradient theorem [23]. After collecting m independent trajectories

$\{(s_t^i, a_t^i, r_t^i)\}_{t=0}^T\}_{i=1}^m$, we can estimate $f(x, y)$ by

$$\hat{f}(x, y) = \frac{1}{m} \sum_{i=1}^m \sum_{t=0}^T \gamma^t r_t^i. \quad (4)$$

And given estimates $\hat{Q}_x(s, a; y)$ to the state-action value function $Q(s, a)$ (assuming an MDP with y as a fixed opponent of x), we can construct an estimator for $\nabla_x f(x, y)$ (and similarly for $\nabla_y f$) by

$$\hat{\nabla}_x f(x, y) \propto \frac{1}{m} \sum_{i=1}^m \sum_{t=0}^T \nabla_x \log \pi_x(a_t^i | s_t^i) \hat{Q}_x(s_t^i, a_t^i; y). \quad (5)$$

4 Convergence Analysis

We establish an asymptotic convergence result in the Monte Carlo policy gradient setting in Thm. 2 for a variant of Alg. 1 under regularity assumptions. This algorithm variant sets $l = 1$ and uses the vanilla SGD as the policy optimizer. We add a stop criterion $\hat{f}(x_i^k, v^k) - \hat{f}(u^k, y_i^k) \lesssim \epsilon$ after Line 6 with an accuracy parameter ϵ . The full proof can be found in the supplementary. Since the algorithm is symmetric between agents in the population, we drop the subscript i for text clarity.

Assumption 1. $X, Y \subseteq \mathbb{R}^d$ are compact sets. As a consequence, there exists D s.t. $\forall x_1, x_2 \in X$, $\|x_1 - x_2\|_1 \leq D$ and $\forall y_1, y_2 \in Y$, $\|y_1 - y_2\|_1 \leq D$. C_y^k, C_x^k are compact subsets of X and Y . Further, assume $f: X \times Y \mapsto \mathbb{R}$ is a bounded convex-concave function.

Theorem 1 (Convergence with exact gradients [15]). *Under A1, assume a sequence $(x^k, y^k) \rightarrow (\hat{x}, \hat{y}) \wedge f(x^k, v^k) - f(u^k, y^k) \rightarrow 0$ implies (\hat{x}, \hat{y}) is a saddle point, Alg. 1 (replacing all estimates with true values) produces a sequence of points $\{(x^k, y^k)\}_{k=0}^\infty$ convergent to a saddle.*

The above case with exact sub-gradients is easy since both f and ∇f are deterministic. In RL setting, we construct estimates for $f(x, y)$ (Eq. 4) and $\nabla_x f, \nabla_y f$ (Eq. 5) with samples. The intuition is that, when the samples are large enough, we can bound the deviation between the true values and estimates by concentration inequalities, then the proof outline similar to [15] also goes through.

Thm. 2 requires an extra assumption on the boundedness of \hat{Q} and gradients. By showing the policy gradient estimates are approximate sub-/super-gradients of f , we are able to prove that the output (x_i^N, y_i^N) of Alg. 1 is an approximate Nash equilibrium with high probability.

Assumption 2. *The Q value estimation \hat{Q} is unbiased and bounded by R , and the policy has bounded gradient $\|\nabla \log \pi_\theta(a|s)\|_\infty \leq B$.*

Theorem 2 (Convergence with policy gradients). *Under A1, A2, let sample size at step k be $m_k \geq \Omega\left(\frac{R^2 B^2 D^2}{\epsilon^2} \log \frac{d}{\delta 2^{-k}}\right)$ and learning rate $\eta_k = \alpha \frac{\bar{E}_k - 2\epsilon}{\|\hat{g}_x^k\|^2 + \|\hat{g}_y^k\|^2}$ with $0 \leq \alpha \leq 2$, then with probability at least $1 - \mathcal{O}(\delta)$, the Monte Carlo version of Alg. 1 generates a sequence of points $\{(x^k, y^k)\}_{k=0}^\infty$ convergent to an $\mathcal{O}(\epsilon)$ -approximate equilibrium (\bar{x}, \bar{y}) , that is $\forall x \in X, \forall y \in Y, f(x, \bar{y}) - \mathcal{O}(\epsilon) \leq f(\bar{x}, \bar{y}) \leq f(\bar{x}, y) + \mathcal{O}(\epsilon)$.*

Discussion. The theorems require f to be convex in x and concave in y , but not strictly. This is a weaker assumption than Arrow-Hurwicz-Uzawa's [13]. The purpose of this simple analysis is mainly a sanity check and an assurance of the correctness of our method. It applies to the setting in Sec. 5.1 but not beyond, as the assumptions do not necessarily hold for neural networks. The sample size is chosen loosely as we are not aiming at a sharp finite sample complexity or regret analysis. In practice, we can find empirically suitable m_k (sample size) and η_k (learning rates), and adopt a modern RL algorithm with an advanced optimizer (e.g., PPO [37] with RmsProp [38]) in place of the SGD updates.

5 Experiments

We empirically evaluate our algorithm on several games with distinct characteristics. The implementation is based on PyTorch. Code, details, and demos are in the supplementary material.

Compared methods. In Matrix games, we compare to a naive mirror descent method, which is essentially Self-play with the latest agent. In the rest of the environments, we compare the results of the following methods:

1. **Self-play with the latest agent (Arrow-Hurwicz-Uzawa).** The learner always competes with the most recent agent. This is essentially the Arrow-Hurwicz-Uzawa method [13] or the naive mirror/alternating descent.
2. **Self-play with the best past agent.** The learner competes with the best historical agent maintained. The new agent replaces the best agent if it beats the previous one. This is the scheme in AlphaGo Zero and AlphaZero [2, 3].
3. **Self-play with a random past agent (Fictitious play).** The learner competes against a randomly sampled historical opponent. This is the scheme in OpenAI sumo [5, 10]. It is similar to Fictitious play [18] since uniformly random sampling is equivalent to historical average by definition. However, Fictitious play only guarantees convergence of the average-iterate but not the last-iterate agent.
4. **OURS**($n = 2, 4, 6, \dots$). This is our algorithm with a population of n pairs of agents trained simultaneously, with each other as candidate opponents. Implementation can be distributed.

Evaluation protocols. We mainly measure the strength of agents by the Elo scores [39]. Pairwise competition results are gathered from a large tournament among *all* the checkpoint agents of all methods after training. Each competition has multiple matches to account for randomness. The Elo scores are computed by logistic regression, as Elo assumes a logistic relationship $P(A \text{ wins}) + 0.5P(\text{draw}) = 1/(1+10^{\frac{R_B - R_A}{400}})$. A 100 Elo difference corresponds to roughly 64% win-rate. The initial agent’s Elo is calibrated to 0. Another way to measure the strength is to compute the average rewards (win-rates) against other agents. We also report average rewards in the supplementary.

5.1 Matrix games

We verified the last-iterate convergence to Nash equilibrium in several classical two-player zero-sum matrix games. In comparison, the vanilla mirror descent/ascent is known to produce oscillating behaviors [31]. Payoff matrices (for both players separated by comma), phase portraits, and error curves are shown in Tab. 1,2,3,4 and Fig. 1,2,3,4. Our observations are listed beside the figures.

We studied two settings: (1) OURS(Exact Gradient), the full information setting, where the players know the payoff matrix and compute the exact gradients on action probabilities; (2) OURS(Policy Gradient), the reinforcement learning or bandit setting, where each player only receives the reward of its own action. The action probabilities were modeled by a probability vector $p \in \Delta_2$. We estimated the gradient w.r.t p with the REINFORCE estimator [40] with sample size $m_k = 1024$, and applied $\eta_k = 0.03$ constant learning rate SGD with proximal projection onto Δ_2 . We trained $n = 4$ agents jointly for Alg. 1 and separately for the naive mirror descent under the same initialization.

5.2 Grid-world soccer game

We conducted experiments in a grid-world soccer game. Similar games were adopted in [41, 24]. Two players compete in a 6×9 grid world, starting from random positions. The action space is {up, down, left, right, noop}. Once a player scores a goal, it gets positive reward 1.0, and the game ends. Up to $T = 100$ timesteps are allowed. The game ends with a draw if time runs out. The game has imperfect information, as the two players move simultaneously.

The policy and value functions were parameterized by simple one-layer networks, consisting of a one-hot encoding layer and a linear layer that outputs the action logits and values. The logits are transformed into probabilities via softmax. We used Advantage Actor-Critic (A2C) [42] with Generalized Advantage Estimation (GAE) [43] and RmsProp [38] as the base RL algorithm. The hyper-parameters are $N = 50$, $l = 10$, $m_k = 32$ for Alg. 1. We kept track of the per-agent number of trajectories (episodes) each algorithm uses for fair comparison. Other hyper-parameters are in the supplementary. All methods were run multiple times to calculate the confidence intervals.

In Fig. 5, OURS($n = 2, 4, 6$) all perform better than others, achieving higher Elo scores after experiencing the same number of per-agent episodes. Other methods fail to beat the rule-based agent after 32000 episodes. Competing with a random past agent learns the slowest, suggesting that, though it may stabilize training and lead to diverse behaviors [5], the learning efficiency is not as high because a large portion of samples is devoted to weak opponents. Within our methods, the performance increases with a larger n , suggesting a larger population may help find better perturbations.

Game payoff matrix

	Heads	Tails
Heads	1, -1	-1, 1
Tails	-1, 1	1, -1

Table 1: Matching Pennies, a classical game where two players simultaneously turn their pennies to heads or tails. If the pennies match, Player 2 wins one penny from 1; otherwise, Player 1 wins. $(P_x(\text{head}), P_y(\text{head})) = (\frac{1}{2}, \frac{1}{2})$ is the unique Nash equilibrium with game value 0.

Phase portraits and error curves

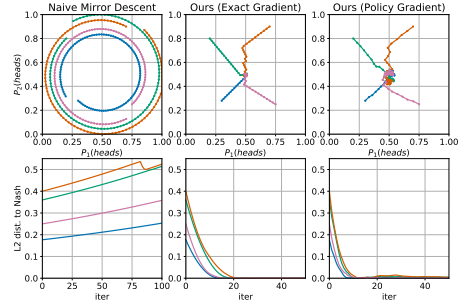


Figure 1: Matching Pennies. (Top) The phase portraits. (Bottom) The squared L_2 distance to the equilibrium. Four colors correspond to 4 agents in the population.

	Heads	Tails
Heads	2, -2	0, 0
Tails	-1, 1	2, -2

Table 2: Skewed Matching Pennies.

Observation: In the leftmost column of Fig. 1,2, the naive mirror descent does not converge (pointwisely); instead, it is trapped in a cyclic behavior. The trajectories of the probabilities of playing Heads orbit around the Nash, showing as circles in the phase portrait. On the other hand, our method enjoys approximate last-iterate convergence with both exact and policy gradients.

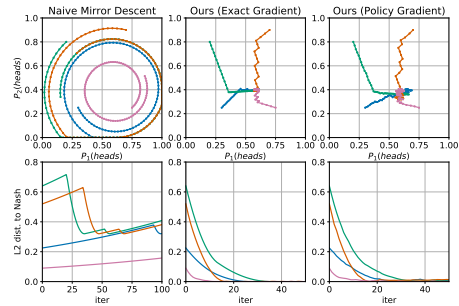


Figure 2: Skewed Matching Pennies. The unique Nash equ. is $(P_x(\text{heads}), P_y(\text{heads})) = (\frac{3}{5}, \frac{2}{5})$ with value 0.8.

	Rock	Paper	Scissors
Rock	0, 0	-1, 1	1, -1
Paper	1, -1	0, 0	-1, 1
Scissors	-1, 1	1, -1	0, 0

Table 3: Rock Paper Scissors.

Observation: Similar observations occur in the Rock Paper Scissors (Fig. 3). The naive method circles around the corresponding equilibrium points $(\frac{3}{5}, \frac{2}{5})$ and $(\frac{1}{3}, \frac{1}{3}, \frac{1}{3})$, while our method converges.

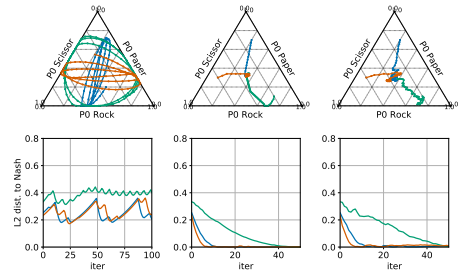


Figure 3: Rock Paper Scissors. (Top) Visualization of Player 1's strategies of one agent P0 from the population. (Down) The squared distance to equilibrium.

	a	b	c
A	1, -1	-1, 1	0.5, -0.5
B	-1, 1	1, -1	-0.5, 0.5

Table 4: Extended Matching Pennies.

Observation: Our method has the benefit of producing diverse solutions when there exist multiple Nash equilibria. The solution for row player is $x = (\frac{1}{2}, \frac{1}{2})$, while any interpolation between $(\frac{1}{2}, \frac{1}{2}, 0)$ and $(0, \frac{1}{3}, \frac{2}{3})$ is an equilibrium column strategy. Depending on initialization, agents in our method converges to different equilibria.

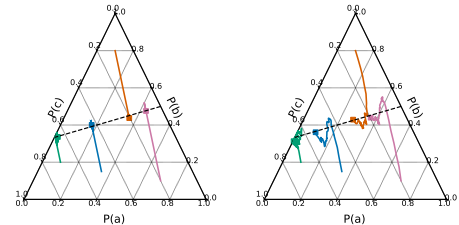


Figure 4: Visualization of Player 2's strategies. (Left) Exact gradient; (Right) Policy gradient. The dashed line represents possible equilibrium strategies. The four agents (in different colors) of the population in our algorithm ($n = 4$) converge differently.

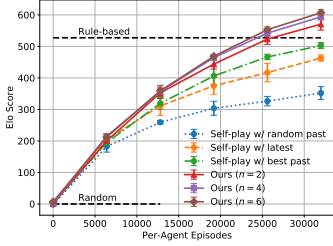


Figure 5: Soccer Elo curves averaged over 3 runs (seeds). For OURS(n), the average is over $3n$ agents. Horizontal lines show the scores of the rule-based and the random-action agents.

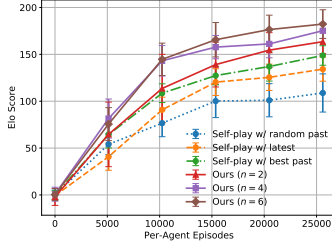


Figure 6: Gomoku Elo curves averaged over 10 runs for the baseline methods, 6 runs (12 agents) for OURS($n = 2$), 4 runs (16 agents) for OURS($n = 4$), and 3 runs (18 agents) for OURS($n = 6$).

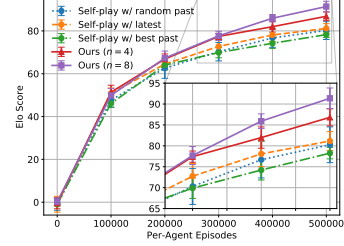


Figure 7: RoboSumo Ants Elo curves averaged over 4 runs for the baseline methods, 2 runs for OURS($n = 4, 8$). A close-up is also drawn for better viewing.

* In all three figures, bars show the 95% confidence intervals. We compare *per-agent* sample efficiency.

5.3 Gomoku board game

We investigated the effectiveness in the Gomoku game, which is also known as Renju, Five-in-a-row. In our variant, two players place black or white stones on a 9-by-9 board in turn. The player who gets an unbroken row of five horizontally, vertically, or diagonally, wins (reward 1). The game is a draw (reward 0) when no valid move remains. The game is sequential and has perfect information.

This experiment involved much more complex neural networks than before. We adopted a 4-layer convolutional ReLU network (kernels (5, 5, 3, 1), channels (16, 32, 64, 1), all strides 1) for both the policy and value networks. Gomoku is hard to train from scratch with pure model-free RL without explicit tree search. Hence, we pre-trained the policy nets on expert data collected from renjuoffline.com. We downloaded roughly 130 thousand games and applied behavior cloning. The pre-trained networks were able to predict expert moves with $\approx 41\%$ accuracy and achieve an average score of 0.93 (96% win and 4% lose) against a random-action player. We adopted the A2C [42] with GAE [43] and RmsProp with learning rate $\eta_k = 0.001$. Up to $N = 40$ iterations of Alg. 1 were run. The other hyperparameters are the same as those in the soccer game.

In Fig. 6, all methods are able to improve upon the behavior cloning policies significantly. OURS($n = 2, 4, 6$) demonstrate higher sample efficiency by achieving higher Elo ratings than the alternatives given the same amount of per-agent experience. This again suggests that the opponents are chosen more wisely, resulting in better policy improvements. Lastly, the more complex policy and value functions (multi-layer CNN) do not seem to undermine the advantage of our approach.

5.4 RoboSumo Ants

Our last experiment is based on the RoboSumo simulation environment in [10, 5], where two Ants wrestle in an arena. This setting is particularly relevant to practical robotics research, as we believe success in this simulation could be transferred into the real-world. The Ants move simultaneously, trying to force the opponent out of the arena or onto the floor. The physics simulator is MuJoCo [44]. The observation space and action space are continuous. This game is challenging since it involves a complex continuous control problem with sparse rewards. Following [10, 5], we utilized PPO [37] with GAE [43] as the base RL algorithm, and used a 2-layer fully connected network with width 64 for function approximation. Hyper-parameters $N = 50, m_k = 500$. In [10], a random past opponent is sampled in self-play, corresponding to the “Self-play w/ random past” baseline here. The agents are initialized from imitating the pre-trained agents of [10]. We consider $n = 4$ and $n = 8$ in our method. From Fig. 7, we observe again that OURS($n = 4, 8$) outperform the baseline methods by a statistical margin and that our method benefits from a larger population size.

6 Conclusion

We propose a new algorithmic framework for competitive self-play policy optimization inspired by a perturbation subgradient method for saddle points. Our algorithm provably converges in convex-concave games and achieves better per-agent sample efficiency in several experiments. In the future, we hope to study a larger population size (should we have sufficient computing power) and the possibilities of model-based and off-policy self-play RL under our framework.

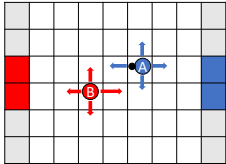
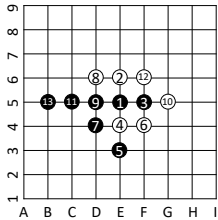
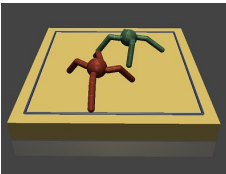
References

- [1] D. Silver, A. Huang, C. J. Maddison, A. Guez, L. Sifre, G. Van Den Driessche, J. Schrittwieser, I. Antonoglou, V. Panneershelvam, M. Lanctot, et al. Mastering the game of go with deep neural networks and tree search. *Nature*, 529(7587):484, 2016. 1, 2, 3
- [2] D. Silver, J. Schrittwieser, K. Simonyan, I. Antonoglou, A. Huang, A. Guez, T. Hubert, L. Baker, M. Lai, A. Bolton, et al. Mastering the game of go without human knowledge. *Nature*, 550(7676):354, 2017. 1, 2, 6
- [3] D. Silver, T. Hubert, J. Schrittwieser, I. Antonoglou, M. Lai, A. Guez, M. Lanctot, L. Sifre, D. Kumaran, T. Graepel, et al. A general reinforcement learning algorithm that masters chess, shogi, and go through self-play. *Science*, 362(6419):1140–1144, 2018. 1, 6
- [4] B. Baker, I. Kanitscheider, T. Markov, Y. Wu, G. Powell, B. McGrew, and I. Mordatch. Emergent tool use from multi-agent autocurricula. In *International Conference on Learning Representations*, 2020. 1
- [5] T. Bansal, J. Pachocki, S. Sidor, I. Sutskever, and I. Mordatch. Emergent complexity via multi-agent competition. *ICLR*, 2017. 1, 6, 8
- [6] M. Jaderberg, W. Czarnecki, I. Dunning, L. Marris, G. Lever, A. Castaneda, C. Beattie, N. Rabinowitz, A. Morcos, A. Ruderman, et al. Human-level performance in 3d multiplayer games with population-based reinforcement learning. *Science*, 364(6443):859–865, 2019. 1
- [7] C. Berner, G. Brockman, B. Chan, V. Cheung, P. Debiak, C. Dennison, D. Farhi, Q. Fischer, S. Hashme, C. Hesse, et al. Dota 2 with large scale deep reinforcement learning. *arXiv preprint arXiv:1912.06680*, 2019. 1
- [8] O. Vinyals, I. Babuschkin, W. M. Czarnecki, M. Mathieu, A. Dudzik, J. Chung, D. H. Choi, R. Powell, T. Ewalds, P. Georgiev, et al. Grandmaster level in starcraft ii using multi-agent reinforcement learning. *Nature*, 575(7782):350–354, 2019. 1
- [9] N. Brown and T. Sandholm. Superhuman ai for multiplayer poker. *Science*, 365(6456):885–890, 2019. 1, 2
- [10] M. Al-Shedivat, T. Bansal, Y. Burda, I. Sutskever, I. Mordatch, and P. Abbeel. Continuous adaptation via meta-learning in nonstationary and competitive environments. In *International Conference on Learning Representations*, 2018. 1, 6, 8
- [11] S. Liu, G. Lever, J. Merel, S. Tunyasuvunakool, N. Heess, and T. Graepel. Emergent coordination through competition. *ICLR*, 2019. 1
- [12] J. Nash. Non-cooperative games. *Annals of mathematics*, pages 286–295, 1951. 2
- [13] K. J. Arrow, H. Azawa, L. Hurwicz, and H. Uzawa. *Studies in linear and non-linear programming*, volume 2. Stanford University Press, 1958. 2, 3, 5, 6
- [14] G. Korpelevich. The extragradient method for finding saddle points and other problems. *Mathematica*, 12:747–756, 1976. 2, 3, 4
- [15] M. Kallio and A. Ruszczyński. Perturbation methods for saddle point computation. 1994. 2, 3, 5, 14, 15
- [16] A. Nedić and A. Ozdaglar. Subgradient methods for saddle-point problems. *Journal of optimization theory and applications*, 2009. 2, 3
- [17] M. Zinkevich, M. Johanson, M. Bowling, and C. Piccione. Regret minimization in games with incomplete information. In *Advances in neural information processing systems*, pages 1729–1736, 2008. 2, 3
- [18] G. W. Brown. Iterative solution of games by fictitious play. *Activity analysis of production and allocation*, 13(1):374–376, 1951. 2, 6
- [19] S. Singh, M. Kearns, and Y. Mansour. Nash convergence of gradient dynamics in general-sum games. *UAI*, 2000. 2
- [20] A. Nowé, P. Vrancx, and Y.-M. De Hauwere. Game theory and multi-agent reinforcement learning. *Reinforcement Learning*, page 441, 2012. 2
- [21] J. Heinrich and D. Silver. Deep reinforcement learning from self-play in imperfect-information games. *arXiv:1603.01121*, 2016. 2, 3
- [22] A. Jafari, A. Greenwald, D. Gondek, and G. Ercal. On no-regret learning, fictitious play, and nash equilibrium. *ICML*, 2001. 2

- [23] R. Sutton and A. Barto. *reinforcement learning: an introduction*. MIT press, 2018. 2, 4
- [24] M. L. Littman. Markov games as a framework for multi-agent reinforcement learning. In *Machine Learning*, pages 157–163. Elsevier, 1994. 2, 6
- [25] G. Tesauro. Temporal difference learning and td-gammon. *Communications of the ACM*, 38(3):58–68, 1995. 2
- [26] J. Hu and M. P. Wellman. Nash q-learning for general-sum stochastic games. *JMLR*, 4(Nov):1039–1069, 2003. 2
- [27] M. Bowling and M. Veloso. Multiagent learning using a variable learning rate. *Artificial Intelligence*, 136(2):215–250, 2002. 2
- [28] Y. Bai and C. Jin. Provable self-play algorithms for competitive reinforcement learning. *arXiv preprint arXiv:2002.04017*, 2020. 2
- [29] M. Lanctot, V. Zambaldi, A. Gruslys, A. Lazaridou, K. Tuyls, J. Pérolat, D. Silver, and T. Graepel. A unified game-theoretic approach to multiagent reinforcement learning. In *Advances in neural information processing systems*, pages 4190–4203, 2017. 2
- [30] A. R. Cardoso, J. Abernethy, H. Wang, and H. Xu. Competing against nash equilibria in adversarially changing zero-sum games. In *International Conference on Machine Learning*, pages 921–930, 2019. 2
- [31] P. Mertikopoulos, H. Zenati, B. Lecouat, C.-S. Foo, V. Chandrasekhar, and G. Piliouras. Optimistic mirror descent in saddle-point problems: Going the extra (gradient) mile. *ICLR*, 2019. 2, 3, 4, 6
- [32] S. Rakhlin and K. Sridharan. Optimization, learning, and games with predictable sequences. In *Advances in Neural Information Processing Systems*, pages 3066–3074, 2013. 2
- [33] J. Hamm and Y.-K. Noh. K-beam minimax: Efficient optimization for deep adversarial learning. *ICML*, 2018. 3
- [34] A. Gleave, M. Dennis, C. Wild, N. Kant, S. Levine, and S. Russell. Adversarial policies: Attacking deep reinforcement learning. In *International Conference on Learning Representations*, 2019. 3
- [35] J.-B. Grill, F. Altché, Y. Tang, T. Hubert, M. Valko, I. Antonoglou, and R. Munos. Monte-carlo tree search as regularized policy optimization. *ICML*, 2020. 3
- [36] L. S. Shapley. Stochastic games. *PNAS*, 39(10):1095–1100, 1953. 3
- [37] J. Schulman, F. Wolski, P. Dhariwal, A. Radford, and O. Klimov. Proximal policy optimization algorithms. *arXiv preprint arXiv:1707.06347*, 2017. 5, 8
- [38] G. Hinton, N. Srivastava, and K. Swersky. Neural networks for machine learning lecture 6a overview of mini-batch gradient descent. 5, 6
- [39] A. E. Elo. *The rating of chessplayers, past and present*. Arco Pub., 1978. 6
- [40] R. J. Williams. Simple statistical gradient-following algorithms for connectionist reinforcement learning. *Machine learning*, 8(3-4):229–256, 1992. 6
- [41] H. He, J. Boyd-Graber, K. Kwok, and H. Daumé III. Opponent modeling in deep reinforcement learning. *ICML*, 2016. 6
- [42] V. Mnih, A. P. Badia, M. Mirza, A. Graves, T. Lillicrap, T. Harley, D. Silver, and K. Kavukcuoglu. Asynchronous methods for deep reinforcement learning. In *ICML*, pages 1928–1937, 2016. 6, 8
- [43] J. Schulman, P. Moritz, S. Levine, et al. High-dimensional continuous control using generalized advantage estimation. *ICLR*, 2016. 6, 8
- [44] E. Todorov, T. Erez, and Y. Tassa. Mujoco: A physics engine for model-based control. In *2012 IEEE/RSJ International Conference on Intelligent Robots and Systems*, pages 5026–5033. IEEE, 2012. 8

A Experiment details

A.1 Illustrations of the games in the experiments

Illustration	Properties
	<p>Figure 8: Illustration of the 6x9 grid-world soccer game. Red and blue represent the two teams A and B. At start, the players are initialized to random positions on respective sides, and the ball is randomly assigned to one team. Players move up, down, left and right. Once a player scores a goal, the corresponding team wins and the game ends. One player can intercept the other’s ball by crossing the other player.</p> <p>Observation: Tensor of shape $[5,]$, $(x_A, y_A, x_B, y_B, A \text{ has ball})$</p> <p>Action: {up, down, left, right, noop}</p> <p>Time limit: 50 moves</p> <p>Terminal reward: +1 for winning team -1 for losing team 0 if timeout</p>
	<p>Figure 9: Illustration of the Gomoku game (also known as Renju, five-in-a-row). We study the 9x9 board variant. Two players sequentially place black and white stones on the board. Black goes first. A player wins when he or she gets five stones in a row. In the case of this illustration, the black wins because there is five consecutive black stones in the 5th row. Numbers in the stones indicate the ordered they are placed.</p> <p>Observation: Tensor of shape $[9, 9, 3]$, last dim 0: vacant, 1: black, 2: white</p> <p>Action: Any valid location on the 9x9 board</p> <p>Time limit: 41 moves per-player</p> <p>Terminal reward: +1 for winning player -1 for losing player 0 if timeout</p>
	<p>Figure 10: Illustration of the RoboSumo Ants game. Two ants fight in the arena. The goal is to push the opponent out of the arena or down to the floor. Agent positions are initialized to be random at the start of the game. The game ends in a draw if the time limit is reached. In addition to the terminal ± 1 reward, the environment comes with shaping rewards (motion bonus, closeness to opponent, etc.). In order to make the game zero-sum, we take the difference between the original rewards of the two ants.</p> <p>Observation: R^{120}</p> <p>Action: R^8</p> <p>Time limit: 100 moves</p> <p>Reward: $r_t = r_t^{\text{orig } y} - r_t^{\text{orig } x}$ Terminal ± 1 or 0.</p>

A.2 Hyper-parameters

The hyper-parameters in different games are listed in Tab. 5.

A.3 Additional results

Win-rates (or average rewards). Here we report additional results in terms of the average win-rates, or equivalently the average rewards through the linear transform $\text{win-rate} = 0.5 + 0.5 \text{ reward}$, in Tab. 6 and 7. Since we treat each (x_i, y_i) pair as one agent, the values are the average of $f(x_i, \cdot)$ and $f(\cdot, y_i)$ in the first table. The one-side $f(\cdot, y_i)$ win-rates are in the second table. Mean and 95%

Table 5: Hyper-parameters.

Hyper-param \ Game	Soccer	Gomoku	RoboSumo
Num. of iterations N	50	40	50
Learning rate η_k	0.1	$0 \rightarrow 0.001$ in first 20 steps then 0.001	$3e-5 \rightarrow 0$ linearly
Value func learning rate	(Same as above.)	(Same as above.)	9e-5
Sample size m_k	32	32	500
Num. of inner updates l	10	10	10
Env. time limit	50	41 per-player	100
Base RL algorithm	A2C	A2C	PPO, clip 0.2, mini-batch 512, epochs 3
Optimizer	RmsProp, $\alpha = 0.99$	RmsProp, $\alpha = 0.99$	RmsProp, $\alpha = 0.99$
Max gradient norm	1.0	1.0	0.1
GAE λ parameter	0.95	0.95	0.98
Discounting factor γ	0.97	0.97	0.995
Entropy bonus coef.	0.01	0.01	0
Policy function	Sequential[OneHot[5832], Linear[5832,5], Softmax, CategoricalDist]	Sequential[Conv[c16,k5,p2], ReLU, Conv[c32,k5,p2], ReLU, Conv[c64,k3,p1], ReLU, Conv[c1,k1], Spatial Softmax, CategoricalDist]	Sequential[Linear[120,64], TanH, Linear[64,64], TanH, Linear[64,8], TanH, GaussianDist] Tanh ensures the mean of the Gaussian is between -1 and 1. The density is corrected.
Value function	Sequential[OneHot[5832], Linear[5832,1]]	Share 3 Conv layers with the policy, but additional heads: global average and Linear[64,1]	Sequential[Linear[120,64], TanH, Linear[64,64], TanH, Linear[64,1]]

confidence intervals are estimated from multiple runs. Exact numbers of runs are in the captions of Fig. 5,6,7 of the main paper. The message is the same as that suggested by the Elo scores: Our method consistently produces stronger agents. We hope the win-rates may give better intuition about the relative performance of different methods.

Training time. Thanks to the easiness of parallelization, the proposed algorithm enjoys good scalability. We can either distribute the n agents into n processes to run concurrently, or make the roll-outs parallel. Our implementation took the later approach. In the most time-consuming RoboSumo Ants experiment, with 30 Intel Xeon CPUs, the baseline methods took approximately 2.4h, while Ours (n=4) took 10.83h to train ($\times 4.5$ times), and Ours (n=8) took 20.75h ($\times 8.6$ times). Note that, Ours (n) trains n agents simultaneously. If we train n agents with the baseline methods by repeating the experiment n times, the time would be $2.4n$ hours, which is comparable to Ours (n).

Chance of selecting the agent itself as opponent. One big difference between our method and the compared baselines is the ability to select opponents adversarially from the population. Consider the agent pair (x_i, y_i) . When training x_i , our method finds the strongest opponent (that incurs the largest loss on x_i) from the population, whereas the baselines always choose (possibly past versions of) y_i . Since the candidate set contains y_i , the “fall-back” case is to use y_i as opponent in our method. We report the frequency that y_i is chosen as opponent for x_i (and x_i for y_i likewise). This gives a sense of how often our method falls back to the baseline method. From Tab. 8, we can observe that, as n

Table 6: Average win-rates ($\in [0, 1]$) between the last-iterate (final) agents trained by different algorithms. Last two rows further show the average over other last-iterate agents and all other agents (historical checkpoint) included in the tournament, respectively. Since an agent consists of an (x, y) pair, the win-rate is averaged on x and y , i.e., $\text{win}(\text{col vs row}) = \frac{f(x^{\text{row}}, y^{\text{col}}) - f(x^{\text{col}}, y^{\text{row}})}{2} \times 0.5 + 0.5$. The lower the better within each column; The higher the better within each row.

(a) Soccer						
Soccer	Self-play latest	Self-play best	Self-play rand	Ours (n=2)	Ours (n=4)	Ours (n=6)
Self-play latest	-	0.533 \pm 0.044	0.382 \pm 0.082	0.662 \pm 0.054	0.691 \pm 0.029	0.713 \pm 0.032
Self-play best	0.467 \pm 0.044	-	0.293 \pm 0.059	0.582 \pm 0.042	0.618 \pm 0.031	0.661 \pm 0.030
Self-play rand	0.618 \pm 0.082	0.707 \pm 0.059	-	0.808 \pm 0.039	0.838 \pm 0.028	0.844 \pm 0.043
Ours (n=2)	0.338 \pm 0.054	0.418 \pm 0.042	0.192 \pm 0.039	-	0.549 \pm 0.022	0.535 \pm 0.022
Ours (n=4)	0.309 \pm 0.029	0.382 \pm 0.031	0.162 \pm 0.028	0.451 \pm 0.022	-	0.495 \pm 0.023
Ours (n=6)	0.287 \pm 0.032	0.339 \pm 0.030	0.156 \pm 0.043	0.465 \pm 0.022	0.505 \pm 0.023	-
Last-iter average	0.357 \pm 0.028	0.428 \pm 0.028	0.202 \pm 0.023	0.532 \pm 0.023	0.608 \pm 0.018	0.585 \pm 0.022
Overall average	0.632 \pm 0.017	0.676 \pm 0.014	0.506 \pm 0.020	0.749 \pm 0.009	0.775 \pm 0.006	0.776 \pm 0.008

(b) Gomoku						
Gomoku	Self-play latest	Self-play best	Self-play rand	Ours (n=2)	Ours (n=4)	Ours (n=6)
Self-play latest	-	0.523 \pm 0.026	0.462 \pm 0.032	0.551 \pm 0.024	0.571 \pm 0.018	0.576 \pm 0.017
Self-play best	0.477 \pm 0.026	-	0.433 \pm 0.031	0.532 \pm 0.024	0.551 \pm 0.018	0.560 \pm 0.020
Self-play rand	0.538 \pm 0.032	0.567 \pm 0.031	-	0.599 \pm 0.027	0.588 \pm 0.022	0.638 \pm 0.020
Ours (n=2)	0.449 \pm 0.024	0.468 \pm 0.024	0.401 \pm 0.027	-	0.528 \pm 0.015	0.545 \pm 0.017
Ours (n=4)	0.429 \pm 0.018	0.449 \pm 0.018	0.412 \pm 0.022	0.472 \pm 0.015	-	0.512 \pm 0.013
Ours (n=6)	0.424 \pm 0.017	0.440 \pm 0.020	0.362 \pm 0.020	0.455 \pm 0.017	0.488 \pm 0.013	-
Last-iter average	0.455 \pm 0.010	0.479 \pm 0.011	0.407 \pm 0.012	0.509 \pm 0.010	0.537 \pm 0.008	0.560 \pm 0.008
Overall average	0.541 \pm 0.004	0.561 \pm 0.004	0.499 \pm 0.005	0.583 \pm 0.004	0.599 \pm 0.003	0.615 \pm 0.003

(c) RoboSumo					
RoboSumo	Self-play latest	Self-play best	Self-play rand	Ours (n=4)	Ours (n=8)
Self-play latest	-	0.502 \pm 0.012	0.493 \pm 0.013	0.511 \pm 0.011	0.510 \pm 0.010
Self-play best	0.498 \pm 0.012	-	0.506 \pm 0.014	0.514 \pm 0.008	0.512 \pm 0.010
Self-play rand	0.507 \pm 0.013	0.494 \pm 0.014	-	0.508 \pm 0.011	0.515 \pm 0.011
Ours (n=4)	0.489 \pm 0.011	0.486 \pm 0.008	0.492 \pm 0.011	-	0.516 \pm 0.008
Ours (n=8)	0.490 \pm 0.010	0.488 \pm 0.010	0.485 \pm 0.011	0.484 \pm 0.008	-
Last-iter average	0.494 \pm 0.006	0.491 \pm 0.005	0.492 \pm 0.006	0.500 \pm 0.005	0.514 \pm 0.005
Overall average	0.531 \pm 0.004	0.527 \pm 0.004	0.530 \pm 0.004	0.539 \pm 0.003	0.545 \pm 0.003

Table 7: Average *one-sided* win-rates ($\in [0, 1]$) between the last-iterate (final) agents trained by different algorithms. The win-rate is one-sided, i.e., $\text{win}(y^{\text{col}} \text{ vs } x^{\text{row}}) = f(x^{\text{row}}, y^{\text{col}}) \times 0.5 + 0.5$. The lower the better within each column; The higher the better within each row.

(a) Soccer						
row $x \setminus$ col y	Self-play latest	Self-play best	Self-play rand	Ours (n=2)	Ours (n=4)	Ours (n=6)
Self-play latest	0.536 \pm 0.054	0.564 \pm 0.079	0.378 \pm 0.103	0.674 \pm 0.080	0.728 \pm 0.039	0.733 \pm 0.048
Self-play best	0.497 \pm 0.065	0.450 \pm 0.064	0.306 \pm 0.106	0.583 \pm 0.056	0.601 \pm 0.039	0.642 \pm 0.050
Self-play rand	0.614 \pm 0.163	0.719 \pm 0.090	0.481 \pm 0.102	0.796 \pm 0.071	0.816 \pm 0.039	0.824 \pm 0.062
Ours (n=2)	0.350 \pm 0.051	0.419 \pm 0.057	0.181 \pm 0.049	0.451 \pm 0.037	0.525 \pm 0.031	0.553 \pm 0.034
Ours (n=4)	0.346 \pm 0.046	0.365 \pm 0.047	0.140 \pm 0.034	0.427 \pm 0.034	0.491 \pm 0.020	0.494 \pm 0.033
Ours (n=6)	0.308 \pm 0.042	0.319 \pm 0.052	0.136 \pm 0.050	0.483 \pm 0.043	0.505 \pm 0.030	0.515 \pm 0.032
Last-iter average	0.381 \pm 0.033	0.422 \pm 0.036	0.188 \pm 0.028	0.525 \pm 0.029	0.601 \pm 0.021	0.587 \pm 0.026
Overall average	0.654 \pm 0.017	0.665 \pm 0.016	0.502 \pm 0.021	0.745 \pm 0.010	0.771 \pm 0.006	0.775 \pm 0.009

(b) Gomoku						
row $x \setminus$ col y	Self-play latest	Self-play best	Self-play rand	Ours (n=2)	Ours (n=4)	Ours (n=6)
Self-play latest	0.481 \pm 0.031	0.540 \pm 0.038	0.488 \pm 0.050	0.594 \pm 0.041	0.571 \pm 0.026	0.586 \pm 0.030
Self-play best	0.494 \pm 0.033	0.531 \pm 0.030	0.471 \pm 0.049	0.597 \pm 0.040	0.562 \pm 0.024	0.572 \pm 0.028
Self-play rand	0.565 \pm 0.036	0.605 \pm 0.036	0.572 \pm 0.051	0.668 \pm 0.040	0.617 \pm 0.027	0.647 \pm 0.029
Ours (n=2)	0.491 \pm 0.031	0.533 \pm 0.033	0.470 \pm 0.040	0.568 \pm 0.035	0.571 \pm 0.022	0.552 \pm 0.025
Ours (n=4)	0.428 \pm 0.022	0.461 \pm 0.024	0.440 \pm 0.035	0.515 \pm 0.029	0.491 \pm 0.017	0.503 \pm 0.020
Ours (n=6)	0.435 \pm 0.021	0.453 \pm 0.026	0.370 \pm 0.028	0.462 \pm 0.025	0.479 \pm 0.018	0.467 \pm 0.017
Last-iter average	0.472 \pm 0.012	0.506 \pm 0.014	0.438 \pm 0.017	0.549 \pm 0.016	0.550 \pm 0.011	0.564 \pm 0.012
Overall average	0.548 \pm 0.005	0.585 \pm 0.005	0.536 \pm 0.007	0.631 \pm 0.006	0.608 \pm 0.004	0.617 \pm 0.004

(c) RoboSumo					
row $x \setminus$ col y	Self-play latest	Self-play best	Self-play rand	Ours (n=4)	Ours (n=8)
Self-play latest	0.516 \pm 0.022	0.494 \pm 0.020	0.491 \pm 0.023	0.502 \pm 0.017	0.511 \pm 0.016
Self-play best	0.489 \pm 0.018	0.504 \pm 0.023	0.503 \pm 0.022	0.506 \pm 0.014	0.509 \pm 0.014
Self-play rand	0.505 \pm 0.021	0.491 \pm 0.026	0.494 \pm 0.026	0.518 \pm 0.017	0.516 \pm 0.014
Ours (n=4)	0.480 \pm 0.018	0.479 \pm 0.012	0.502 \pm 0.016	0.496 \pm 0.009	0.517 \pm 0.012
Ours (n=8)	0.491 \pm 0.012	0.484 \pm 0.016	0.485 \pm 0.016	0.486 \pm 0.012	0.491 \pm 0.012
Last-iter average	0.489 \pm 0.008	0.485 \pm 0.008	0.495 \pm 0.009	0.500 \pm 0.007	0.514 \pm 0.007
Overall average	0.528 \pm 0.004	0.521 \pm 0.004	0.530 \pm 0.005	0.534 \pm 0.003	0.544 \pm 0.003

grows larger, the chance of fall-back is decreased. This is understandable since a larger population means larger candidate sets and a larger chance to find good perturbations.

Table 8: Average frequency of using the agent itself as opponent, in the Soccer and Gomoku experiments. The frequency is calculated by counting over all agents and iterations. The \pm shows the *standard deviations* estimated by 3 runs with different random seeds.

Method	Ours ($n = 2$)	Ours ($n = 4$)	Ours ($n = 6$)
Frequency of self (Soccer)	0.4983 \pm 0.0085	0.2533 \pm 0.0072	0.1650 \pm 0.0082
Frequency of self (Gomoku)	0.5063 \pm 0.0153	0.2312 \pm 0.0111	0.1549 \pm 0.0103

B Proofs

We adopt the following variant of Alg. 1 in our asymptotic convergence analysis. For clarity, we investigate the learning process of one agent in the population and drop the i index. C_x^k and C_y^k are not set simply as the population for the sake of the proof. Alternatively, we pose some assumptions. Setting them to the population as in the main text may approximately satisfy the assumptions.

Algorithm 2: Simplified perturbation-based self-play policy optimization of one agent.

Input: η_k : learning rates, m_k : sample size;

Result: Pair of policies (x, y) ;

```

1 Initialize  $x^0, y^0$ ;
2 for  $k = 0, 1, 2, \dots \infty$  do
3   Construct candidate opponent sets  $C_y^k$  and  $C_x^k$ ;
4   Find perturbed  $v^k = \arg \max_{y \in C_y^k} \hat{f}(x^k, y)$  and perturbed  $u^k = \arg \min_{x \in C_x^k} \hat{f}(x, y^k)$  where the
   evaluation is done with Eq. 4 and sample size  $m_k$ ;
5   Compute estimated duality gap  $\hat{E}_k = \hat{f}(x^k, v^k) - \hat{f}(u^k, y^k)$ ;
6   if  $\hat{E}_k \leq 3\epsilon$  then
7     | return  $(x^k, y^k)$ 
8   Estimate policy gradients  $\hat{g}_x^k = \hat{\nabla}_x f(x^k, v^k)$  and  $\hat{g}_y^k = \hat{\nabla}_y f(u^k, y^k)$  w/ Eq. 5 and sample size  $m_k$ ;
9   Update policy parameters with  $x^{k+1} \leftarrow x^k - \eta_k \hat{g}_x^k$  and  $y^{k+1} \leftarrow y^k + \eta_k \hat{g}_y^k$ ;
```

B.1 Proof of Theorem 1

We restate the assumptions and the theorem here more clearly for reference.

Assumption B.1. $X, Y \subseteq \mathbb{R}^d$ ($d > 1$) are compact sets. As a consequence, there exists $D \geq 1$, s.t.,

$$\forall x_1, x_2 \in X, \|x_1 - x_2\|_1 \leq D \text{ and } \forall y_1, y_2 \in Y, \|y_1 - y_2\|_1 \leq D.$$

Further, assume $f: X \times Y \mapsto \mathbb{R}$ is a bounded convex-concave function.

Assumption B.2. C_y^k, C_x^k are compact subsets of X and Y . Assume that a sequence $(x^k, y^k) \rightarrow (\hat{x}, \hat{y}) \wedge f(x^k, v^k) - f(u^k, y^k) \rightarrow 0$ for some $v^k \in C_y^k$ and $u^k \in C_x^k$ implies (\hat{x}, \hat{y}) is a saddle point.

Theorem 1 (Convergence with exact gradients [15]). *Under Assump. B.1, B.2, let the learning rate satisfies*

$$\eta_k < \frac{E_k}{\|g_x^k\|^2 + \|g_y^k\|^2},$$

Alg. 2 (when replacing all estimates with true values) produces a sequence of points $\{(x^k, y^k)\}_{k=0}^\infty$ convergent to a saddle point.

Assump. B.1 is standard, which is true if f is based on a payoff table and X, Y are probability simplex as in matrix games, or if f is quadratic and X, Y are unit-norm vectors. Assump. B.2 is about the regularity of the candidate opponent sets. This is true if C_y^k, C_x^k are compact and $f(x^k, v^k) - f(u^k, y^k) = 0$ only at a saddle point $(u^k, v^k) \in C_y^k \times C_x^k$. An trivial example would

be $C_x^k = X, C_y^k = Y$. Another example would be the proximal regions around x^k, y^k . In practice, Alg. 1 constructs the candidate sets from the population which needs to be adequately large and diverse to satisfy Assump. B.2 approximately.

The proof is due to [15], which we paraphrase here.

Proof. We shall prove that one iteration of Alg. 2 decreases the distance between the current (x^k, y^k) and the optimal (x^*, y^*) . Expand the squared distance,

$$\|x^{k+1} - x^*\|^2 \leq \|x^k + \eta_k g_x^k - x^*\|^2 = \|x^k - x^*\|^2 + 2\eta_k \langle g_x^k, x^k - x^* \rangle + \eta_k^2 \|g_x^k\|^2. \quad (6)$$

From Assump. B.1, convexity of $f(x, y)$ on x gives

$$\langle g_x^k, x^k - x^* \rangle \geq f(x^k, v^k) - f(x^*, v^k) \quad (7)$$

which yields

$$\|x^{k+1} - x^*\|^2 \leq \|x^k - x^*\|^2 - 2\eta_k (f(x^k, v^k) - f(x^*, v^k)) + \eta_k^2 \|g_x^k\|^2. \quad (8)$$

Similarly for y^k , concavity of $f(x, y)$ on y gives

$$\|y^{k+1} - y^*\|^2 \leq \|y^k - y^*\|^2 + 2\eta_k (f(u^k, y^k) - f(u^k, y^*)) + \eta_k^2 \|g_y^k\|^2. \quad (9)$$

Sum the two and notice the saddle point condition implies

$$f(x^*, v^k) \leq f(x^*, y^*) \leq f(u^k, y^*), \quad (10)$$

we have

$$\begin{aligned} W_{k+1} &:= \|x^{k+1} - x^*\|^2 + \|y^{k+1} - y^*\|^2 \\ &\leq \|x^k - x^*\|^2 + \|y^k - y^*\|^2 \\ &\quad - 2\eta_k \left(f(x^k, v^k) - f(x^*, v^k) - f(u^k, y^k) + f(u^k, y^*) \right) + \eta_k^2 (\|g_x^k\|^2 + \|g_y^k\|^2) \\ &\leq W_k - 2\eta_k E_k + \eta_k^2 (\|g_x^k\|^2 + \|g_y^k\|^2). \end{aligned} \quad (11)$$

If the learning rate satisfies $\eta_k < \frac{E_k}{\|g_x^k\|^2 + \|g_y^k\|^2}$, the sequence $\{W_k\}_{k=0}^\infty$ is strictly decreasing unless $E_k = 0$. Since W_k is bounded below by 0, therefore $E_k \rightarrow 0$. Following from Assump. B.2, the convergent point $\lim_{k \rightarrow \infty} (x_k, y_k) = (x^*, y^*)$ is a saddle point. \square

B.2 Proof of Theorem 2

We restate the additional Assump. B.3 and the theorem here for reference. Assump. B.2 is replaced by the following approximated version B.4.

Assumption B.3. The total return is bounded by R , i.e., $|\sum_t \gamma^t r_t| \leq R$. The Q value estimator \hat{Q} is unbiased and bounded by R ($|\hat{Q}| \leq R$). And the policy has bounded gradient $\max\{\|\nabla \log \pi_\theta(a|s)\|_\infty, 1\} \leq B$ in terms of L_∞ norm.

Assumption B.4. C_y^k, C_x^k are compact subsets of X and Y . Assume at iteration k , for some $(\hat{x}, \hat{y}) \in X \times Y$,

$$\forall (u, v) \in C_x^k \times C_y^k, f(u, \hat{y}) - \epsilon \leq f(\hat{x}, \hat{y}) \leq f(\hat{x}, v) + \epsilon$$

implies

$$\forall (u, v) \in X \times Y, f(u, \hat{y}) - \epsilon \leq f(\hat{x}, \hat{y}) \leq f(\hat{x}, v) + \epsilon,$$

namely, (\hat{x}, \hat{y}) is an ϵ -approximate saddle point.

Theorem 2 (Convergence with policy gradients). *Under Assump. B.1, B.3, B.4, let sample size at step k be*

$$m_k \geq \frac{2R^2 B^2 D^2}{\epsilon^2} \log \frac{2d}{\delta^{2-k}}$$

and, with $0 \leq \alpha \leq 2$, let the learning rate

$$\eta_k = \alpha \frac{\hat{E}_k - 2\epsilon}{\|\hat{g}_x^k\|^2 + \|\hat{g}_y^k\|^2}.$$

Then with probability at least $1 - \mathcal{O}(\delta)$, the Monte Carlo version of Alg. 2 generates a sequence of points $\{(x^k, y^k)\}_{k=0}^{\infty}$ convergent to an $\mathcal{O}(\epsilon)$ -approximate equilibrium (\bar{x}, \bar{y}) . That is

$$\forall x \in X, \forall y \in Y, \quad f(x, \bar{y}) - \mathcal{O}(\epsilon) \leq f(\bar{x}, \bar{y}) \leq f(\bar{x}, y) + \mathcal{O}(\epsilon).$$

In the stochastic game (or reinforcement learning) setting, we construct estimates for $f(x, y)$ (Eq. 4) and policy gradients $\nabla_x f, \nabla_y f$ (Eq. 5) with samples. Intuitively speaking, when the samples are large enough, we can bound the deviation between the true values and the estimates by concentration inequalities, then the similar proof outline also goes through.

Let us first define the concept of ϵ -subgradient for convex functions and ϵ -supergradient for concave functions. Then we calculate how many samples are needed for accurate gradient estimation in Lemma 3 with high probability. With Lemma 3, we will be able to show that the Monte Carlo policy gradient estimates are good enough to be ϵ -subgradients when sample size is large in Lemma 4.

Definition 1. An ϵ -subgradient of a convex function $h : \mathbb{R}^d \mapsto \mathbb{R}$ at x is $g \in \mathbb{R}^d$ that satisfies

$$\forall x', h(x') - h(x) \geq \langle g, x' - x \rangle - \epsilon.$$

Similarly, an ϵ -supergradient of a concave function $h : \mathbb{R}^d \mapsto \mathbb{R}$ at x is $g \in \mathbb{R}^d$ that satisfies

$$\forall x', h(x') - h(x) \leq \langle g, x' - x \rangle + \epsilon.$$

Lemma 3 (Policy gradient sample size). *Consider x or y alone and treat the problem as MDP. Suppose Assump. B.3 is satisfied. Then with independently collected*

$$m \geq \frac{2R^2 B^2}{\epsilon^2} \log \frac{2d}{\delta}$$

trajectories $\{(s_t^i, a_t^i, \hat{Q}_t^i)\}_{t=0}^T\}_{i=1}^m$, the policy gradient estimate

$$\widehat{\nabla} f = \frac{1}{m} \sum_{i,t} \nabla \log \pi_{\theta}(a_t^i | s_t^i) \hat{Q}_t^i$$

is ϵ -close to the true gradient ∇f with high probability, namely,

$$\Pr(\|\widehat{\nabla} f - \nabla f\|_{\infty} \leq \epsilon) \geq 1 - \delta.$$

Proof. It directly follows from Hoeffding's inequality and the union bound, since the range of each sample point is bounded by RB and by the policy gradient theorem $\mathbb{E}\widehat{\nabla} f = \nabla f$. \square

Lemma 4 (Policy gradients are ϵ sub-/super- gradients). *Under Assump. B.1, the policy gradient estimate $\widehat{\nabla}_x f$ in Lemma 3 is an ϵD -subgradient of f at x , i.e., for all $x' \in X$,*

$$f(x', y) - f(x, y) \geq \langle \widehat{\nabla}_x f, x' - x \rangle - \epsilon D$$

with probability $\geq 1 - \delta$. (And $\widehat{\nabla}_y f$ is ϵD -super-gradient for y .)

Proof. Apply the telescoping trick,

$$\begin{aligned} \langle \widehat{\nabla}_x f, x' - x \rangle &= \langle \widehat{\nabla}_x f - \nabla_x f + \nabla_x f, x' - x \rangle \\ &= \langle \nabla_x f, x' - x \rangle + \langle \widehat{\nabla}_x f - \nabla_x f, x' - x \rangle \\ &\geq f(x', y) - f(x, y) + \langle \widehat{\nabla}_x f - \nabla_x f, x' - x \rangle. \end{aligned} \quad (12)$$

With the sample size in Lemma 3, we know it holds that $\max_i |\widehat{\nabla}_x f - \nabla_x f|_i \leq \epsilon$ with probability $\geq 1 - \delta$. Hence, by Holder's inequality, the last part satisfies

$$\langle \widehat{\nabla}_x f - \nabla_x f, x' - x \rangle \geq -\langle |\widehat{\nabla}_x f - \nabla_x f|, |x' - x| \rangle \geq -\|\widehat{\nabla}_x f - \nabla_x f\|_{\infty} \|x' - x\|_1 \geq -\epsilon D. \quad (13)$$

The proof of $\widehat{\nabla}_y f$ being ϵD -super-gradient for y is similar, hence omitted. \square

Similarly for accurate function value evaluation, we have the following lemma on sample size, which directly follows from Hoeffding's inequality.

Lemma 5 (Evaluation sample size). *Suppose Assump. B.3 holds. Then with independently collected $m \geq \frac{2R^2}{\epsilon^2} \log \frac{2}{\delta}$ trajectories $\{(s_t^i, a_t^i, r_t^i)\}_{t=0}^T\}_{i=1}^m$, the value estimate $\hat{f} = \frac{1}{m} \sum_{i,t} \gamma^t r_t$ is ϵ -close to the true gradient f with high probability, namely, $\Pr(\|\hat{f} - f\|_\infty \leq \epsilon) \geq 1 - \delta$.*

Now we prove our main theorem which guarantees the output of Alg. 2 is an approximate Nash with high probability. This is done by using Lemma 4 in place of the exact convexity condition to analyze the relationship between W_k and W_{k+1} , using Lemma 5 to bound the error of policy evaluation, and analyzing the stop condition carefully.

Proof. (Theorem 2.)

Suppose (x^*, y^*) is one saddle point of f . We shall prove that one iteration of Alg. 2 sufficiently decreases the squared distance between the current (x^k, y^k) and (x^*, y^*) defined as $W_k := \|x^k - x^*\|^2 + \|y^k - y^*\|^2$.

Relation between W_k and W_{k+1} :

Note that

$$W_{k+1} = \|x^{k+1} - x^*\|^2 \leq \|x^k + \eta_k \hat{g}_x^k - x^*\|^2 = \|x^k - x^*\|^2 + 2\eta_k \langle \hat{g}_x^k, x^k - x^* \rangle + \eta_k^2 \|\hat{g}_x^k\|^2. \quad (14)$$

By Lemma 4, the gradient estimate \hat{g}_x^k with sample size m_k is an ϵ -subgradient on x with probability at least $1 - \delta/2^k$, i.e.,

$$\langle \hat{g}_x^k, x^k - x^* \rangle \geq f(x^k, v^k) - f(x^*, v^k) - \epsilon. \quad (15)$$

Plugging back into Eq. 14, we get

$$\|x^{k+1} - x^*\|^2 \leq \|x^k - x^*\|^2 - 2\eta_k (f(x^k, v^k) - f(x^*, v^k) - \epsilon) + \eta_k^2 \|\hat{g}_x^k\|^2. \quad (16)$$

Similarly for y^k , since \hat{g}_x^k is a super-gradient by Lemma 4,

$$\|y^{k+1} - y^*\|^2 \leq \|y^k - y^*\|^2 + 2\eta_k (f(u^k, y^k) - f(u^k, y^*) + \epsilon) + \eta_k^2 \|\hat{g}_y^k\|^2. \quad (17)$$

Sum the two inequalities above, and notice the saddle point condition implies

$$f(x^*, v^k) \leq f(x^*, y^*) \leq f(u^k, y^*),$$

we have the following inequality holds with probability $1 - 2\delta/2^k$,

$$\begin{aligned} W_{k+1} &= \|x^{k+1} - x^*\|^2 + \|y^{k+1} - y^*\|^2 \\ &\leq \|x^k - x^*\|^2 + \|y^k - y^*\|^2 \\ &\quad - 2\eta_k (f(x^k, v^k) - f(x^*, v^k) - f(u^k, y^k) + f(u^k, y^*) - 2\epsilon) + \eta_k^2 (\|\hat{g}_x^k\|^2 + \|\hat{g}_y^k\|^2) \\ &\leq W_k - 2\eta_k (E_k - 2\epsilon) + \eta_k^2 (\|\hat{g}_x^k\|^2 + \|\hat{g}_y^k\|^2). \end{aligned} \quad (18)$$

Accurate estimation of E_k : In Eq. 18, the second term involves E_k which is unknown to the algorithm. Recall that $E_k(u^k, v^k) = f(x^k, v^k) - f(u^k, y^k)$ and the empirical estimate $\hat{E}_k = \hat{f}(x^k, v^k) - \hat{f}(u^k, y^k)$ in Alg. 2 Line 5.

By Lemma 5, when the sample size m_k is chosen as in Theorem 2, with probability $1 - \frac{2\delta}{d2^k}$,

$$|\hat{f}(x^k, v^k) - f(x^k, v^k)| \leq \frac{\epsilon}{BD} \leq \epsilon$$

and

$$|\hat{f}(u^k, y^k) - f(u^k, y^k)| \leq \frac{\epsilon}{BD} \leq \epsilon.$$

Thus \hat{E}_k is 2ϵ -accurate because

$$\begin{aligned} \hat{E}_k - 2\epsilon &= f(x^k, v^k) - \epsilon - f(u^k, y^k) - \epsilon \leq E_k \\ &\leq f(x^k, v^k) + \epsilon - f(u^k, y^k) + \epsilon = \hat{E}_k + 2\epsilon. \end{aligned} \quad (19)$$

Case (1). Stop condition in Alg. 2 Line 6: If there does not exist $(u, v) \in C_x^k \times C_y^k$ such that $\hat{E}_k(u, v) > 3\epsilon$, meaning $\forall (u, v) \in C_x^k \times C_y^k, \hat{E}_k \leq 3\epsilon$. We can conclude

$$E_k = f(x^k, v) - f(u, y^k) \leq \hat{E}_k + 3\epsilon = 5\epsilon \quad (20)$$

with probability at least $1 - \frac{2\delta}{d2^k} \geq 1 - \frac{2\delta}{2^k}$.

Set $v = y^k$ and $u = x^k$ respectively in the above inequality, we obtain $\forall (u, v) \in C_x^k \times C_y^k$,

$$f(u, y^k) - 5\epsilon \leq f(x^k, y^k) \leq f(x^k, v) + 5\epsilon. \quad (21)$$

Following from Assump. B.4, this implies $\forall (u, v) \in X \times Y, f(u, y^k) - 5\epsilon \leq f(x^k, y^k) \leq f(x^k, v) + 5\epsilon$, which suggests (x^k, y^k) is an approximate saddle point (equilibrium).

On the other hand, we want to bound the failure probability. Define events

$$F(g) := “|\hat{g} - g| \leq \epsilon \text{ is true}”$$

for all $g \in \{g_x^0, g_y^0, f(x^0, v^0), f(u^0, y^0) \dots, g_y^k, f(x^k, y^k) \dots\}$. By De Morgan’s law and the union bound,

$$\begin{aligned} & \Pr [\text{all MC estimates till step } k \text{ are } \epsilon \text{ accurate}] \\ &= \Pr \left[\bigcap_{l=0}^k F(g_x^l) \cap F(g_y^l) \cap F(f(x^l, v^l)) \cap F(f(u^l, y^l)) \right] \\ &= 1 - \Pr \left[\bigcup_{l=1}^k \overline{F(g_x^l) \cap \dots \cap F(f(u^l, y^l))} \right] \\ &\geq 1 - \mathcal{O} \left(\sum_{l=0}^{\infty} \frac{\delta}{2^l} \right) \\ &\geq 1 - \mathcal{O}(\delta). \end{aligned} \quad (22)$$

This means that inaccurate MC estimation (failure) occurs with small probability $\mathcal{O}(\delta)$. The purpose of the increasing m_k w.r.t. k is to handle the union bound and the geometric series here. So, when the algorithm stops, it returns $(\bar{x}, \bar{y}) = (x_k, y_k)$ as a 5ϵ -approximate solution to the saddle point (equilibrium) with high probability.

Case (2). Sufficient decrease of W_k : Otherwise, if the stop condition is not triggered, we have picked u^k, v^k such that $\hat{E}_k > 3\epsilon$. With probability $1 - 2\delta$, $E_k > \hat{E}_k - 2\epsilon \geq \epsilon$. With the chosen learning rate η_k in the theorem statement, W_k strictly decreases by at least

$$W_k - W_{k+1} > \frac{\alpha(2-\alpha)\epsilon^2}{\|\hat{g}_x^k\|^2 + \|\hat{g}_y^k\|^2} \geq \frac{\alpha(2-\alpha)\epsilon^2}{2R^2B^2} > 0. \quad (23)$$

Since W_k is bounded below by 0, by the monotone convergence theorem, there exists a finite k such that $W_0 \leq k \frac{\alpha(2-\alpha)\epsilon^2}{2R^2B^2}$, and no (u, v) can be found to decrease W_k more than 3ϵ . In this case, $\forall (u, v) \in C_x^k \times C_y^k, \hat{E}_k(u, v) \leq 3\epsilon$, which is exactly the stop condition in Case (1). This means the algorithm will eventually stop, and the proof is complete. \square

Remark 1. The sample size is chosen very loosely. More efficient ways to find perturbations (e.g., best-arm identification), to better characterize or cover the policy class and to better utilize trajectories (e.g., especially off-policy evaluation w/ importance sampling) can potentially reduce sample complexity. In practice, we found on-policy methods which do not reuse past experience such as A2C and PPO work well enough.

Remark 2. Assump. B.4 is a rather strong assumption on the candidate opponent sets. In theory, we can construct an ϵ -covering of f to satisfy the assumption. In practice, as in population-based training of Alg. 1, this assumption can be roughly met if n is large or diverse enough. We found a relatively small population with randomly initialized agents already brought noticeable benefit.

Remark 3. The proof requires a variable learning rate η_k . However, the intuition is that the learning rate needs to be small, as we did in our experiments.